Low Contrast Imaging With A GaAs Pixel Digital Detector [1]

S.R. Amendolia[2], M.G. Bisogni[3], U. Bottigli[3], M.A. Ciocci[4], P. Delogu[3], G. Dipasquale[5], M.E. Fantacci[3], M. Giannelli[3], P. Maestro[3], V.M. Marzulli[3], E. Pernigotti[3], V. Rosso[3], A. Stefanini[3], S. Stumbo[2]

[2]Dipartimento di Matematica e Fisica dell'Università, Sassari and Sezione INFN, Pisa, Italy

[3]Dipartimento di Fisica dell'Università and Sezione INFN, Pisa, Italy

[4]Dipartimento di Fisica dell'Università di Siena and Sezione INFN, Pisa, Italy

[5]Dipartimento di Fisica dell'Università and Unità di Ricerca INFM, Pisa, Italy

Abstract

A digital mammography system based on GaAs pixel detector has been developed by the INFN (Istituto Nazionale di Fisica Nucleare) collaboration MED46.

The high atomic number makes the GaAs a very efficient material for low energy X-rays detection ($10 - 30\ keV$ is the typical energy range used in mammography). Low contrast details can be detected with a significant dose reduction to the patient. The system presented in this paper consists of a 4096 pixel matrix built on a 200 μm thick Semi Insulating GaAs substrate. The pixel size is $170 \times 170\ \mu m^2$ for a total active area of $1.18\ cm^2$. The detector is bump-bonded to a VLSI Front-End chip which implements a single-photon counting architecture. This feature allows to enhance the radiographic contrasts detection with respect to charge integrating devices.

The system has been tested by using a standard mammographic tube. Images of mammographic phantoms will be presented and compared with radiographs obtained with traditional film/screen systems. Monte Carlo simulations have been also performed to evaluate the imaging capability of the system. Comparison with simulations and experimental results will be shown.

I. Introduction

Breast cancer is a major problem in disease prevention. It is foreseen that the yearly increment of cases since year 2000 will be around one million [1]. Mammographic screening programs rely consequently on an efficient early diagnosis. It is expected that such a diagnosis can reduce mortality by 30-40 % for ages above 50. The research in mammography aims at an improvement of image quality, which brings over higher sensitivity and specificity in the diagnosis, together with a sensible reduction of the dose, which will favour the extension of the screening to ages below 50.

One of the most promising approaches to this problem is a mammographic imaging system based on GaAs pixel detectors [2]. This kind of detector features a high detection efficiency, namely 98 % compared to 60 % of the conventional film (at the typical 20 keV mammography X-ray energy). It allows the detection of very low contrast ($\leq 3\%$) details with a high precision. The detection of such low contrast structures is the sole weapon to spot early tumoral mass formation.

[1]Corresponding author: Salvator Roberto Amendolia, Università di Sassari and INFN Sezione di Pisa, Via Livornese 1291, I-56010 San Piero a Grado, Pisa (Italy). Fax: +39-050-880317. E_mail: amendolia@pi.infn.it

In the past years the MEDIM collaboration of the INFN developed an X-ray imaging system prototype based on a small GaAs pixel detector and a hybrid read-out electronics, operating in single photon counting mode [3]. The detector has been built on a 200 μm thick GaAs substrate. Its pixel architecture features a matrix of 6×6, 200 μm wide, square pixels with 20 μm electrode spacing. Each pixel is connected to the corresponding electronic channel by means of wire bonding. With this system images of a phantom containing low contrast details have been acquired with a standard mammographic tube.

The main constraint for a pixel detector of significant area has always been the difficulty of a planar arrangement of a large number of channels and the relevant problem of electrical connections. For the 36 channels prototype the sensitive area was only $1.7\ mm^2$. A big step toward the solution of this problem has been offered by the bump-bonding technique. A front-end VLSI integrated circuit is designed with the read-out cells of the same shape and dimensions of the detector pixels. Each electronics cell is connected to the corresponding pixel by means of a metal bump of few tens of microns in diameter [4]. Taking advantage of this technique, the MED46 experiment of INFN and the MEDIPIX collaboration developed the X-ray digital imaging prototype presented in this paper.

II. System Description

This system exploits the advantages of a single-photon-counting technology, which improves the noise performance and the contrast sensitivity compared with conventional charge integrating systems [5, 6].

The pixel detector has been built by ALENIA [7] on a 200 μm thick (SI) Semi Insulating LEC (Liquid Encapsulated Czochralsky) GaAs substrate, by deposition of a 64×64 square Schottky contacts matrix. The electrode area is $150 \times 150\ \mu m^2$ and the electrode separation is 20 μm so that the pixel size is $170 \times 170\ \mu m^2$. The total active area is $1.18\ cm^2$. On the other side of the bulk a large non-alloyed ohmic contact has been built [8, 9].

The Front-End IC (Integrated Circuit), named PCC (Photon Counting Chip), has been realized for the $MEDIPIX$ collaboration by the $CERN$ Microelectronic Group in $SACMOS$ 1 μm technology [10]. The PCC is composed of 64×64 asynchronous readout cells. The pixel size is $170 \times 170\ \mu m^2$ in order to match the detector cell. Each channel of the PCC contains a low noise charge preamplifier, a leading edge comparator with adjustable threshold and a 15–bit

0018-9499/00$10.00

pseudo-random counter. Main feature of this circuit are a fine threshold control (3-bits) for each pixel, a minimum common threshold of 1500 e^- rms with a spread of 100 e^- rms. The average ENC (Equivalent Noise Charge) is about 150 e^- rms. The Front-End IC is bump-bonded to the detector by means of 24 μm in diameter bonding pads. An I/O 16–bit bus has been built to upload the configuration bits and to download the data. The I/O operations can be performed at $10MHz$ and a 64 × 64 pixel image can be read-out in 400 μs.

An external readout system, called MRS (Medipix Readout System) and developed by LABEN [11], manages the PCC set-up and the DAQ (Data Acquisition). A C program has been written to control the readout system MRS [12].

The electronics performance has been measured and the results reported in a previous paper [13].

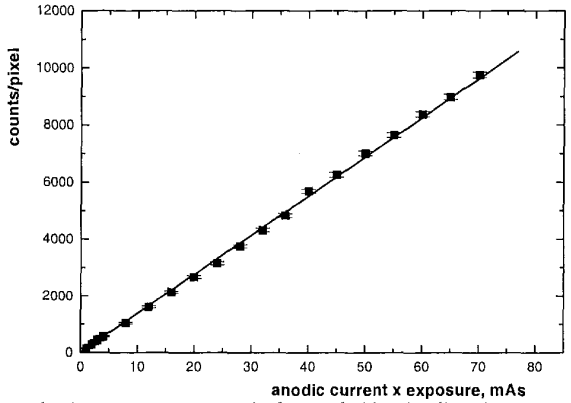

Figure 1: Average counts per pixel recorded by the digital system as a function of the anodic current times exposure time (squares). Linear fit of the data (line).

III. X-RAY IMAGING TESTS

A. Experimental set–up and counting efficiency evaluation

In order to test the imaging capability of our system, a standard mammographic tube [14] has been used. It is equipped with a Mo target, filtration of $0.025\,mm\,Mo + 1\,mm\,Be$. The tube operated at 28 kVp. The flux is $4.67 \times 10^5\ mm^{-2}mAs^{-1}$ at 75 cm from the source. The anodic current times exposure time ranges from 0 to 70 mAs. Figure 1 shows the average counts per pixel as a function of the anodic current times exposure time. The linearity of the system is very good also for high exposure values (the typical range for clinical mammography is $10 - 40\,mAs$).

In figure 2 the energy spectrum of the beam after 4 cm of Lucite ($C_5H_8O_2$, $\rho = 1.18\frac{g}{cm^3}$, $\frac{\mu}{\rho}(20\,keV) = 0.536\frac{cm^2}{g}$) is shown (solid line). The incident flux on the detector is $1.13 \times 10^4\ mm^{-2}mAs^{-1}$ at 75 cm from the beam focus [15]. The same figure also shows the calculated counting efficiency ϵ_{calc} (circles). It has been obtained by convolving the energy spectrum with the GaAs detection efficiency and integrating over the spectrum energy range ($0 - 28\ keV$) to take into account the Front-End energy discrimination threshold. GaAs detection efficiency has been taken according to the Monte

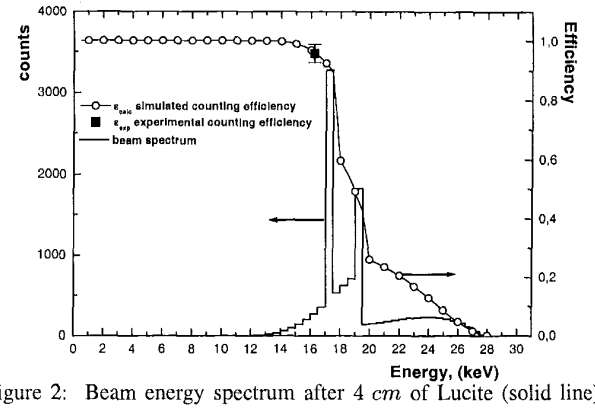

Figure 2: Beam energy spectrum after 4 cm of Lucite (solid line). Simulated counting efficiency convolved with the energy spectrum, ϵ_{calc}, (open circles). Experimental counting efficiency, ϵ_{exp}, (square).

Carlo and experimental data reported in [16, 17]. For the 16.5 keV equivalent threshold, fixed for all the acquisitions, the experimental counting efficiency ϵ_{exp} is $(95.8 \pm 3.0)\%$ (square symbol in figure 2).

B. Simulations

A detailed Monte Carlo simulation, based on the $EGS4$ (Electron Gamma Shower 4) code [18, 19], has been performed. The simulated irradiation geometry is shown in figure 3.

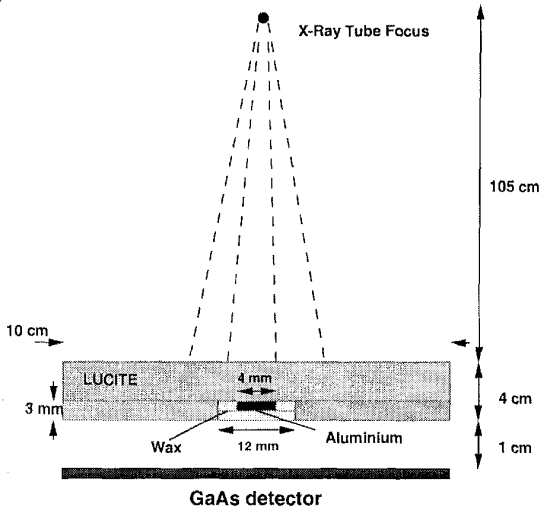

Figure 3: Simulated irradiation geometry.

The beam incident on the phantom is shown in figure 4. The flux is $2.5 \times 10^6\ mm^{-2}$, about one fourth of the clinical standard dose, and the exposed area on the phantom is 3.1 cm^2. The energy distribution of the transmitted photons through the phantom is characterized by an average transmission of about 6% of the incident flux, confirming the high value of the absorbed dose.

The phantom is composed of five Al disks of 4 mm in diameter immersed in wax which in turn is located inside a 10 cm diameter, 4 cm thick Lucite cylinder. The thicknesses of the Al disks are 125 μm, 100 μm, 75 μm, 40 μm, 25 μm.

The simulated detector is a 200 μm thick and 10 cm wide

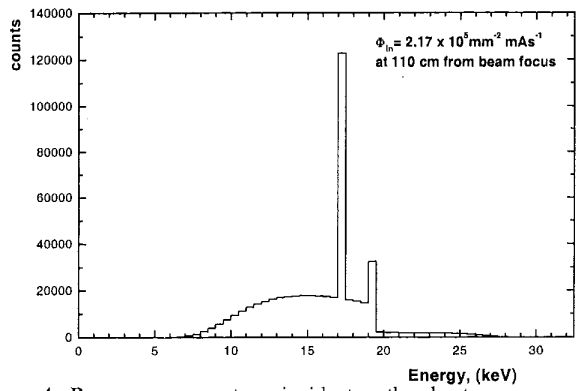

Figure 4: Beam energy spectrum incident on the phantom.

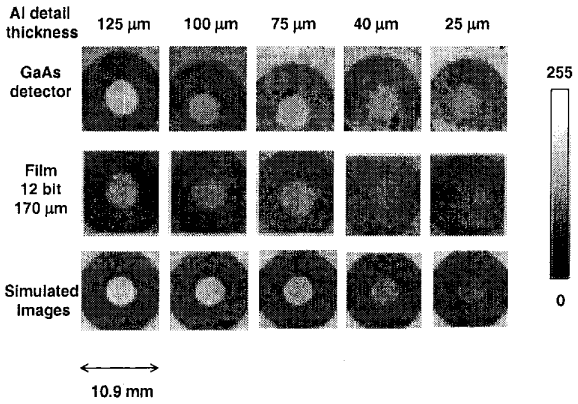

Figure 5: Images of the five aluminium details in the phantom obtained with the digital GaAs system (first row). The same details radiographed by a conventional film/screen system, digitized with a 170 μm pixel size, 12-bit scanner (second row). The images obtained by the simulations (third row). The grey-scale is shown on the right.

GaAs crystal, with a pixel size of $170 \times 170\ \mu m^2$.

In the diagnostic range of mammography the most important interactions are, for photons, the photoelectric effect and the Compton scattering, and, for electrons, the collision energy loss and the multiple scattering. The energy and $X - Y$ coordinates of each event (photon on the phantom surface) are extracted by a random number generator (repetition sequence 10^{43}) according to the X-ray spectrum. Photons and secondary electrons are tracked until they reach the phantom lateral surface or their energy falls respectively below 1 keV and 531 keV. The events which enter the detector are classified as primaries if they did not interact in the phantom, or as secondaries if they have been scattered by the phantom. Electrons and photons release in GaAs for each interaction an energy E_{dep} and a charge sampled from a Gaussian distribution with average value $\overline{Q}_{dep}$:

$$\overline{Q}_{dep} = \frac{E_{dep}}{w} \tag{1}$$

and standard deviation σ :

$$\sigma = \sqrt{F\,\overline{Q}_{dep}} \tag{2}$$

where w is the average energy for electron-hole pair production and F is the Fano factor ($w = 4.2\ eV$ and $F = 0.2$ in GaAs). A detector with complete charge collection has been simulated. For each particle in the crystal the total charge released and the corresponding center-of-mass has been calculated. The single-photon counting mode of the electronics has been reproduced by fixing a threshold of 2500 e^- rms. The event is recorded only if the total charge released in the pixel containing the center-of-mass overcomes the threshold.

C. Mammographic phantom images

A phantom has been built, with precisely known characteristics, in order to determine the real contrast detection capability of the system, and to evaluate the effect of the Compton scattering which contributes to image blurring and artifacts. This phantom has the same geometry as the one used in the Monte Carlo simulation and reproduces a cancer lesion in a 50 % glandular and 50 % adipose breast tissue. The phantom has been placed 105 cm from the beam focus and 1 cm above the detector.

Images of the phantom have been acquired both with the GaAs pixel detector and with a film/screen system dedicated to mammography [20]. Figure 5 shows the images obtained with the digital GaAs system for all these configurations (first row), the images from a conventional film/screen system, digitized with a 170 μm pixel size, 12-bit scanner (second row) and the simulated images (third row). The dimension of the images is 1.18 cm^2 and the pixel size is $170 \times 170\ \mu m^2$. All the experimental images have been obtained with a 32 mAs exposure and an irradiation time of 1 s. The average glandular dose $\overline{D}_g$ given to the phantom to realize an image has been evaluated to be 1 mGy. This value is within the typical range of the dose given to a patient in a clinical mammography.

All the images acquired with the GaAs system have been normalized by means of a weighing matrix to take into account the systematic noise due to the non uniform response of the electronic channels. The radiographs obtained with the pixel detector are qualitatively better than the images acquired with the film/screen system. It is worth to note the capability of our system to detect the image of the 25 μm thick detail while the same detail acquired with film is completely masked by the noise. To make a quantitative comparison of the different

Table 1
Thickness of the radiographed objects (first column). Contrasts measured on the images acquired respectively with the digital system and with the film (second and third columns).

$t\ (\mu m)$	$C_{GaAs}(\%)$	$C_{film}(\%)$
125	7.62 ± 0.13	7.32 ± 0.65
100	6.01 ± 0.13	5.89 ± 0.59
75	4.58 ± 0.14	4.42 ± 0.45
40	2.65 ± 0.18	2.48 ± 0.46
25	1.28 ± 0.19	1.55 ± 0.45

imaging techniques, the contrast [21] of the aluminium details with respect to the wax background have been evaluated and the results have been reported in table 1. In the first column, the thicknesses of the radiographed objects are reported. The

second and third columns show the contrasts measured on the images acquired respectively with the digital system and with the film.

As can be seen, the average contrast values are almost the same for the two imaging techniques but the error on the contrast measure for the film is much higher than for the pixel detector. The film is in fact a charge integrating system and, as shown in [22], its performance in terms of noise and low contrast discrimination is lower with respect to a single photon counting device.

We have simulated the images of the aluminium details taking into account either the contribution of all the events or the one due only to the primaries.

The total contrast C_{total} can be expressed as [21]:

$$C_{total} = \frac{1 - e^{-\Delta\mu \cdot x}}{1 + R} = \frac{C_{pr}}{1 + R} \quad (3)$$

$$R = \frac{secondaries}{primaries} \quad (4)$$

where $\Delta\mu$ is the difference between the linear attenuation coefficients of the aluminium detail and the wax background, x is the detail thickness, R the secondaries over primaries ratio and C_{pr} the contrast due to primaries only. The calculated contrast and the experimental contrast from actual pixel detector acquisitions are shown in table 2. The difference between C_{total} and C_{pr} can be explained by taking into account the secondaries contribution that degrades the image quality. We can also notice the difference between the experimental contrast C_{exp} and the simulated contrast C_{total}. The reason is that, due to computer time limitations, in our simulation the exposed surface was only 3.1 cm^2 instead of 18×24 cm^2 of the experiment, while the value of R depends dramatically on the irradiation area.

Table 2
Contrasts of the simulated images with only primary photons, C_{pr}, and with all the photons (primary and secondary), C_{total}. C_{exp} is experimental value of contrast in the images acquired by the pixel detector.

t (μm)	C_{pr}(%)	C_{total}(%)	C_{exp}(%)
125	11.95 ± 0.15	9.06 ± 0.15	7.62 ± 0.13
100	9.80 ± 0.15	7.24 ± 0.14	6.01 ± 0.13
75	7.28 ± 0.16	5.15 ± 0.15	4.58 ± 0.14
40	3.92 ± 0.16	2.27 ± 0.15	2.65 ± 0.18
25	2.41 ± 0.17	0.98 ± 0.15	1.28 ± 0.19

Finally, figure 6 shows the images of the 125 μm thick Al detail obtained with the conventional film (left side) and with the GaAs detector (right side). The quality of the two images is comparable but the image on the right side has been acquired with one quarter of the dose given to the phantom to realize the left side image. This further demonstrates the advantage of the use of a high efficiency detector over the film/screen system.

IV. Conclusions

The imaging tests conducted in standard mammographic conditions have shown the high performance of the GaAs-based pixel detector system with respect to a mammographic film/screen system in terms of low contrast details detection (the minimum contrast detected with the digital system is 1.28 %) and dose reduction (the minimum dose delivered to the phantom to perform a radiograph with the GaAs detector is 0.25 mGy).

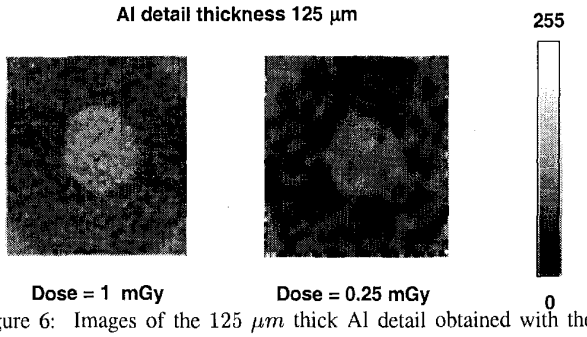

Figure 6: Images of the 125 μm thick Al detail obtained with the traditional film (left side) and with the GaAs detector (right side) with one fourth of the dose. The grey-scale is also shown.

The present work is part of a project funded by INFN and by the Ministry of Research of Italy, as an applied research project. Successful architectural studies, conducted inside the project, together with the results of the imaging tests, presented in this paper, allows us to propose such a system, adequately configured in a large size matrix, as a highly performing mammographic substitute of the conventional film/screen systems.

V. References

[1] American Cancer Society "Cancer Facts and Figures 1994," *American Cancer Society, Atlanta, GA, 1994.*

[2] S.R. Amendolia, M.G. Bisogni, M. Campbell, A. Cola, S. D'Auria, C. Da Via, E.H.M. Heijne, M.E. Fantacci, V. O'Shea, V. Rosso, K. Smith, L. Vasanelli "Experimental Study of LEC GaAs Detectors for X-ray Digital Radiography". *Nucl. Instr. and Meth, A380, 1996*, pp. 410-413.

[3] S.R. Amendolia, E. Bertolucci, M.G. Bisogni, U. Bottigli, M.A. Ciocci, A. Cola, M. Conti, P. Delogu, M.E. Fantacci, G. Magistrati, E. Pernigotti, N. Romeo, P. Russo, A. Stefanini, S. Stumbo, "Imaging performance of a GaAs pixel detector". *Nuovo Cimento A, vol. 112A, no. 1-2, 1999*, pp. 167-177.

[4] S.R. Amendolia, E. Bertolucci, U. Bottigli, M.A. Ciocci, M. Conti, P. Delogu, M.E. Fantacci, G. Magistrati, V. Marzulli, E. Pernigotti, N. Romeo, V. Rosso, P. Russo, A. Stefanini, S. Stumbo, "A project for digital mammography based on a GaAs pixel detector and on a self-triggering single photon counting acquisition system". *Physica Medica, XIII, Suppl. 4, 1997*, pp. 157-165.

[5] M. Sandborg and G.A. Carlsson, "Influence of X–ray energy spectrum, contrasting detail and detector on the signal-to-noise ratio (SNR) and detective quantum efficiency (DQE) in projection radiography", *Phys. Med. Biol., 37(6), 1992* , pp. 1245-1263.

[6] R. Irsigler, J. Andersson, J. Alverbro, J. Borglind, C.

Frojdh, P. Helander, S. Manolopoulos, H. Martijn, V. O'Shea, K. Smith, "X-ray imaging using a 320 × 240 hybrid GaAs pixel detector". *IEEE Trans. Nucl. Sc. Vol 46 (3), 1999*, pp. 507-512.

[7] Alenia S.p.A., Via Tiburtina km 12.4, I-00131 Roma, Italy.

[8] A. Alietti, C. Canali, A. Castaldini, A. Cavallini, A. Cetronio, C. Chiossi, S. D'Auria, C. Del Papa, C. Lanzieri, F. Nava, P. Vanni. "Performance of a new ohmic contact for GaAs radiation detectors". *Nucl. Instr. and Meth, A362, 1995*, pp. 344-348.

[9] S.R. Amendolia, E. Bertolucci, U. Bottigli, M.A. Ciocci, M. Conti, P. Delogu, M.E. Fantacci, P. Maestro, V. Marzulli, N. Romeo, V. Rosso, P. Russo, A. Stefanini. "Charge Collection properties of GaAs detectors for digital radiography". *Physica Medica, XIV, Suppl. 2, 1998*, pp. 17-19.

[10] M.Campbell, E.H.M. Heijne, G. Meddeler, E. Pernigotti, W. Snoeys, "A readout chip for a 64 x 64 pixel matrix with 15-bit single photon counting". *IEEE Trans. Nucl. Sc. Vol 45 (3), 1998*, pp. 751.

[11] Laben S.p.A., Strada Padana Superiore 290, I-20090, Vimodrone (Mi), Italy.

[12] S.R. Amendolia, E. Bertolucci, M.G. Bisogni, U. Bottigli, A. Ceccopieri, M.A. Ciocci, M. Conti, P. Delogu, M.E. Fantacci, P. Maestro, V. Marzulli, E. Pernigotti, N. Romeo, V. Rosso, P. Russo, A. Stefanini, S. Stumbo. "MEDIPIX: a VLSI chip a GaAs pixel detector for digital radiology" *Nucl. Instr. and Meth, A422, 1999*, pp. 201-205.

[13] M.G. Bisogni, M. Campbell, M. Conti, P. Delogu, M. E. Fantacci, E.H.M. Heijne, P. Maestro, G. Magistrati, V. M. Marzulli, G. Meddeler, B. Mikulec, E. Pernigotti, V. Rosso, C. Schwarz, W. Snoeys, S. Stumbo, "Performance of a 4096 Pixel Photon Counting Chip" *Proc. SPIE, Vol. 3445, 1998*, pp. 298-304.

[14] Gilardoni S.p.A., Piazza Luigi di Savoia 28, Milano, Italy.

[15] R. Birch, M. Marshall and G.M. Adran. *Catalogue of spectral Data for Diagnostic X-rays*. London: The Hospital Physicists' Association, 1979.

[16] W. Bencivelli, E. Bertolucci, U. Bottigli, A. Del Guerra, A. Messineo, W.R. Nelson, P. Randaccio, V. Rosso, P. Russo, A. Stefanini, "Evaluation of elemental and compound semiconductors for X-ray digital radiography". *Nucl. Instr. and Meth, A310, 1991*, pp. 210-214.

[17] S.R. Amendolia, M.G. Bisogni, M. Campbell, A. Cola, S. D'Auria, C. Da Vià, E.H.M. Heijne, M.E. Fantacci, V. O'Shea, V. Rosso, K. Smith, L. Vasanelli. "Experimental study of LEC GaAs detectors for X-ray digital radiography". *Nucl. Instr. and Meth, A380, 1996*, pp. 410-413.

[18] W.R. Nelson, H. Hirayama, D.W.O. Rogers. *The EGS4 Code System.* SLAC Report, SLAC-265 1985.

[19] A.F. Bielajew, D.O.W. Rogers. "PRESTA: the Parameter Reduced Electron-Step Transport Algorithm for electron Monte Carlo transport" *Nucl. Instr. and Meth., B18, 1987*, pp. 165-181.

[20] 3M Medical Imaging Film and M Trimatic T ultrafine screen produced by 3M inc.

[21] S.Webb, Physics of medical imaging, Bristol: Adam Hilger, 1989. pp. 20-73.

[22] E. Pernigotti "Comparison between integrating readout systems and single photon counting systems for digital mammography", *Physica Medica, XIV, Suppl. 2, 1998*, pp. 20-22.